Finite-Element Numerical Modeling of Atmospheric Turbulent Boundary Layer

H. N. Lee[1] and S. K. Kao

Department of Meteorology, University of Utah, Salt Lake City 84112

(Manuscript received 14 May 1979, in final form 16 July 1979)

ABSTRACT

A dynamic turbulent boundary-layer model in the neutral atmosphere is constructed, using a dynamic turbulent equation of the eddy viscosity coefficient for momentum derived from the relationship among the turbulent dissipation rate, the turbulent kinetic energy and the eddy viscosity coefficient, with aid of the turbulent second-order closure scheme. A finite-element technique was used for the numerical integration. In preliminary results, the behavior of the neutral planetary boundary layer agrees well with the available data and with the existing elaborate turbulent models, using a finite-difference scheme. The proposed dynamic formulation of the eddy viscosity coefficient for momentum is particularly attractive and can provide a viable alternative approach to study atmospheric turbulence, diffusion and air pollution.

1. Introduction

The numerical modeling of momentum, heat and matter transport in the atmospheric planetary boundary layer (PBL) has been studied extensively by several authors, but primarily air mean motion, mean temperature and mean concentration in matter are computed. In more recent years, a number of turbulence closure theories have been developed and may be found in the works of Deardorff (1970a, b), Hanjalic and Launder (1972), Shir (1973), Mellor (1973), Mellor and Herring (1973), Wyngaard and Coté (1974), Mellor and Yamada (1974), Yamada and Mellor (1975), etc. For a simple first-order closure scheme, mixing-length or eddy-viscosity concepts are generally employed. Here the eddy viscosity coefficients are defined by the ratio of the turbulent shear stress to the mean wind shear. However, uncertainty in the eddy viscosity coefficients still remains a major difficulty in their application. No simple expressions for the eddy viscosity coefficients can be expected to account for the complicated variations of turbulent mixing that occur in the natural atmosphere. Various empirical expressions for the eddy viscosity coefficients have been proposed and they are outlined by Shir and Bornstein (1977). In fact, the distribution of atmospheric turbulent motion over horizontally nonhomogeneous terrain is one important phenomenon which is significantly influenced by the eddy viscosity. There is considerable current interest in this type of turbulent flow over hills. Most of the works on turbulent motion over hills has not been concerned with the effects of stratification (Taylor and Gent, 1974; Frost *et al.*, 1974; Jackson and Hunt, 1975). Although stratification has an important effect on wind over hills, there is lack of a theoretical understanding of turbulent fluxes over horizontally heterogeneous terrain in the PBL even under a neutrally stratified atmosphere. Thus, under neutral conditions this study is only our first step toward a better understanding of turbulent flow over an irregular terrain. Extension of this study to the flow over a low hill terrain is partly studied (Lee, 1979). The model here could be extended to a non-neutral case which is our next step, by the inclusion of the equation of potential temperature. Therefore, the purpose of the present paper is to describe an alternative approach based on dynamic considerations in which the second-order closure is carried over for determining the eddy viscosity coefficients. In the meantime, a finite-element method is employed here for solving the turbulent flows (Baker, 1978; Schamber and Larock, 1978).

Although the second-order closure numerical models have been studied successfully in the turbulence boundary layer, they do not have wide application for the dynamic models in the atmospheric PBL. This is simply because the amount of computer time and storage necessary for the sophisticated turbulence high-order closure models are large and because an adequate comparison between theory and observation has been restricted for lack of enough observed data. In addition, the existing finite-difference techniques have limited usefulness in practical cases in which the terrain is generally not flat. For these reasons the finite-element numerical technique, which is suitable to fit more accurately the irregular geometric boundaries, and the

[1] Present affiliation: Atmospheric Sciences Division, Brookhaven National Laboratory, Upton, NY 11973.

0021-8952/79/101287-09$06.25

simplified turbulence planetary boundary-layer model, which hopefully will yield a realistic approach to give the best agreement with observed data, are proposed in this study.

In a mean turbulence energy computational scheme, encouraging results of prediction of a number of PBL flows were reported by Hanjalic and Launder (1972); as a result the present model has extended their assumptions regarding the third- and second-order correlation terms. Mellor and Yamada's (1974) systematic simplification analysis based on observation is also taken into account by neglecting small order of magnitude terms. In order to solve the model equations with complex geometric boundaries the Galerkin residual finite element is employed.

The finite-element method (Martin and Carey, 1973; Huebner, 1975) is basically a numerical procedure with which continuum problems can be cast in a form which is suitable for solution by digital computers rather quickly and efficiently. Originally, this method using the variational approach was developed for applications in structural mechanics and a voluminous literature was available. Now the method has been refined as the Galerkin-type approach for generating the solution of problems from such diverse areas as heat conduction, fluid dynamics, ground water problems and meteorological problems. The main advantages of this method are a more accurate treatment of boundary conditions, higher accuracy with less numerical diffusion, easy change of parameter properties and accurate representation of complex terrains.

2. General governing equations

We assume that the velocity components and pressure can be expressed as the sum of mean and fluctuating parts. It can be shown that the equations for the mean motion, continuity, Reynolds stress and turbulence dissipation rate at high Reynolds numbers take the forms of

$$\frac{\partial \bar{u}_i}{\partial t}+\bar{u}_j\frac{\partial \bar{u}_i}{\partial x_j}=-\frac{1}{\rho}\frac{\partial \bar{p}}{\partial x_i}+(f_1\epsilon_{3ij}+f_2\epsilon_{2ij})\bar{u}_j$$

$$-g\delta_{3i}+\frac{\mu}{\rho}\frac{\partial^2 \bar{u}_i}{\partial x_j^2}-\frac{\partial(\overline{u_i'u_j'})}{\partial x_j}, \quad (1)$$

$$\frac{\partial \bar{u}_j}{\partial x_j}=0, \quad (2)$$

$$\frac{\partial \overline{u_i'u_k'}}{\partial t}+\bar{u}_j\frac{\partial \overline{u_i'u_k'}}{\partial x_j}=-\overline{u_i'u_j'}\frac{\partial \bar{u}_k}{\partial x_j}-\overline{u_k'u_j'}\frac{\partial \bar{u}_i}{\partial x_j}$$

$$-\frac{\partial}{\partial x_j}\overline{(u_i'u_j'u_k')}-\frac{1}{\rho}\frac{\partial}{\partial x_i}\overline{(p'u_k')}$$

$$-\frac{\partial}{\partial x_k}\overline{(p'u_i')}+\frac{1}{\rho}\left[\overline{p'\left(\frac{\partial u_i'}{\partial x_k}+\frac{\partial u_k'}{\partial x_i}\right)}\right]$$

$$+\frac{\mu}{\rho}\frac{\partial^2\overline{u_i'u_k'}}{\partial x_j^2}-\frac{2\mu}{\rho}\overline{\frac{\partial u_i'}{\partial x_j}\frac{\partial u_k'}{\partial x_j}}, \quad (3)$$

$$\frac{\partial \epsilon}{\partial t}+\bar{u}_j\frac{\partial \epsilon}{\partial x_j}=-2\frac{\mu}{\rho}\frac{\partial \bar{u}_i}{\partial x_k}\left(\overline{\frac{\partial u_i'}{\partial x_m}\frac{\partial u_k'}{\partial x_m}}+\overline{\frac{\partial u_m'}{\partial x_i}\frac{\partial u_m'}{\partial x_k}}\right)$$

$$-2\frac{\mu}{\rho}\overline{\frac{\partial u_i'}{\partial x_k}\frac{\partial u_i'}{\partial x_m}\frac{\partial u_k'}{\partial x_m}}-2\overline{\left(\frac{\mu}{\rho}\frac{\partial^2 u_i'}{\partial x_k\partial x_j}\right)^2}$$

$$-\frac{\mu}{\rho}\frac{\partial}{\partial x_k}\overline{\left(u_k'\frac{\partial u_i'}{\partial x_m}\frac{\partial u_i'}{\partial x_m}\right)}$$

$$-2\frac{\mu}{\rho^2}\frac{\partial}{\partial x_i}\overline{\left(\frac{\partial u_i'}{\partial x_m}\frac{\partial p'}{\partial x_m}\right)}, \quad (4)$$

where g, ρ, μ are gravity force parameter, density and dynamic viscosity; ϵ_{ijk} and δ are the alternating tensors and Kronecker delta; $f_1=2\Omega\sin\phi$ and $f_2=2\Omega\cos\phi$ are Coriolis parameters; and

$$\epsilon=\frac{\mu}{\rho}\overline{\frac{\partial u_i'}{\partial x_m}\frac{\partial u_i'}{\partial x_m}}$$

is the mean rate of turbulence energy dissipation. Here the Coriolis force terms have been neglected in Eqs. (3) and (4) since they are relatively small in the boundary layer (Shir 1973).

For $k=i$, Eq. (3) becomes the turbulence kinetic energy equation

$$\frac{\partial e}{\partial t}+\bar{u}_j\frac{\partial e}{\partial x_j}=-\overline{u_i'u_j'}\frac{\partial \bar{u}_i}{\partial x_j}-\frac{\partial \overline{u_j'e}}{\partial x_j}-\frac{1}{\rho}\frac{\partial}{\partial x_i}\overline{(p'u_i')}$$

$$+\frac{\mu}{\rho}\frac{\partial^2 e}{\partial x_j^2}-\frac{\mu}{\rho}\overline{\frac{\partial u_i'}{\partial x_j}}\,\overline{\frac{\partial u_i'}{\partial x_j}}, \quad (5)$$

where the sum of the normal stresses is equal to twice the turbulence kinetic energy per unit mass, i.e., $2e=\overline{u_i'u_i'}$.

Second-order turbulence closure scheme

It is readily seen from the previous section that if equations for the rate of change of these new variables $\overline{u_i'u_k'}$ and ϵ are constructed more new variables will appear. They contain unknown high order correlation turbulence terms for which closure assumptions must be made in order to solve the problem. In recent years a number of turbulence closure theories have been developed. The basic concept involved in turbulence closure is to provide the closure by modeling the high-order correlations in terms of low-order correlations. The procedure for obtaining second-order closure for the present model is to express high-order correlation terms in the moment equations (3), (4) and (5) in terms of the mean velocities, turbulence dissipation rate, turbulence kinetic energy and the Reynolds stress tensors.

Extending the assumptions of Hanjalic and Launder (1972) and Mellor and Herring (1973) regarding the high-order correlation terms, the equations for the Reynolds stress and turbulence dissipation rate are then

$$\frac{\partial \overline{u_i'u_k'}}{\partial t}+\bar{u}_j\frac{\partial \overline{u_i'u_k'}}{\partial x_j} = -\overline{u_i'u_j'}\frac{\partial \bar{u}_k}{\partial x_j}-\overline{u_k'u_j'}\frac{\partial \bar{u}_i}{\partial x_j}+C_7\frac{\partial}{\partial x_j}\left[\left(\frac{e}{\epsilon}\overline{u_i'u_l'}\frac{\partial \overline{u_j'u_k'}}{\partial x_l}+\overline{u_j'u_l'}\frac{\partial \overline{u_k'u_i'}}{\partial x_l}+\overline{u_k'u_l'}\frac{\partial \overline{u_i'u_j'}}{\partial x_l}\right)\right]-C_1\frac{\epsilon}{e}\left(\overline{u_i'u_k'}-\frac{2e}{3}\delta_{ik}\right)+C_2e\left(\frac{\partial \bar{u}_i}{\partial x_k}+\frac{\partial \bar{u}_k}{\partial x_i}\right)-\tfrac{2}{3}\epsilon\delta_{ik}, \quad (6)$$

$$\frac{\partial \epsilon}{\partial t}+\bar{u}_j\frac{\partial \epsilon}{\partial x_j} = -C_3\frac{\epsilon}{e}\overline{u_i'u_k'}\frac{\partial \bar{u}_i}{\partial x_k}-C_4\frac{\epsilon^2}{e}+C_5\frac{\partial}{\partial x_k}\left(\frac{e}{\epsilon}\overline{u_k'u_m'}\frac{\partial \epsilon}{\partial x_m}\right). \quad (7)$$

The modeling techniques in the Reynolds stress transport equation can also be used for modeling terms in the turbulence kinetic energy transport equation.

3. The model equations

a. Simplification of the governing equations

It may be noticed that the resultant equations in the preceding section form a closed system once the constants C_i in Eqs. (6) and (7) are determined. The main problem, therefore, is to solve 13 simultaneous partial differential equations (three for $\bar{u}_i$, nine for $\overline{u_i'u_k'}$ and one for ϵ). Because there is a practical limitation in the amount of computer time and storage, it is desirable to simplify systematically the full closure model by levels of complexity (Mellor and Yamada, 1974). For instance, the simple version (level 2 modeling approximation) was adopted satisfactorily by Freeman (1977) to study the tensor diffusivity of a trace constituent in a stratified boundary layer. Also, Yamada and Mellor (1975) utilized successfully the complex version (the level 3 modeling approximation) to simulate the Wangara experimental data. Hence, this encouraging systematic simplification analysis by neglecting small order of magnitude terms introduced by Mellor and Yamada (1974) is taken for the analysis, in which the level 3 modeling approximation is chosen in the present model.

For the present study, the turbulence kinetic energy equation is employed instead of solving equations for each of the normal stresses. Therefore, the normal stresses which remain in the equations of the turbulence kinetic energy, Reynolds stress and turbulence dissipation rate are then taken as proportional to the turbulence kinetic energy. They will be shown in a later section. Further, in the two-dimensional boundary-layer flows the shear stresses involving the vertical component of the turbulent velocity ($-\overline{u'w'}$ and $\overline{v'w'}$) are assumed to have the predominant effect on the mean velocity. Thus, the model equations for the turbulence motion in the neutral atmospheric planetary boundary layer can be constructed to give

$$\frac{D\bar{u}}{Dt}=f_1(\bar{v}-\bar{v}_g)-\frac{\partial}{\partial z}(\overline{u'w'}), \quad (8)$$

$$\frac{D\bar{v}}{Dt}=-f_1(\bar{u}-\bar{u}_g)-\frac{\partial}{\partial z}(\overline{v'w'}), \quad (9)$$

$$\frac{\partial \bar{u}}{\partial x}+\frac{\partial \bar{v}}{\partial y}+\frac{\partial \bar{w}}{\partial z}=0, \quad (10)$$

$$-\overline{u'w'}=\left(\frac{C_6-C_2}{C_1}\right)\frac{e^2}{\epsilon}\frac{\partial \bar{u}}{\partial z}, \quad (11)$$

$$\overline{v'w'}=-\left(\frac{C_6-C_2}{C_1}\right)\frac{e^2}{\epsilon}\frac{\partial \bar{v}}{\partial z}, \quad (12)$$

$$\frac{De}{Dt}=-\overline{u'w'}\frac{\partial \bar{u}}{\partial z}-\overline{v'w'}\frac{\partial \bar{v}}{\partial z}+C_6(1+C_6)C_7\frac{\partial}{\partial z}\left(\frac{e^2}{\epsilon}\frac{\partial e}{\partial z}\right)-\epsilon, \quad (13)$$

$$\frac{D\epsilon}{Dt}=-C_3\frac{\epsilon}{e}\left(\overline{u'w'}\frac{\partial \bar{u}}{\partial z}+\overline{v'w'}\frac{\partial \bar{v}}{\partial z}\right)-C_4\frac{\epsilon^2}{e}+C_6C_5\frac{\partial}{\partial z}\left(\frac{e^2}{\epsilon}\frac{\partial \epsilon}{\partial z}\right), \quad (14)$$

where $\bar{u}_g$ and $\bar{v}_g$ are the geostrophic wind components, C_6 is a constant which is the ratio between normal stress ($\overline{w'^2}$) and turbulence kinetic energy (e). Here $D(\ )/Dt=\partial(\ )/\partial t+\bar{u}\partial(\ )/\partial x+\bar{v}\partial(\ )/\partial y+\bar{w}\partial(\ )/\partial z$.

b. Dynamic equation for the eddy viscosity coefficient

Using Eqs. (8)–(14) the atmospheric turbulent structures in the neutral PBL can be studied once the constants C_i are determined. It is seen that this second-order closure model is superior because it does not need any information about eddy viscosity coefficients which is required by the first-order closure model in order to solve the problem. However, treating the regions of rapid vertical variation of turbulence dissipation rate near the surface is a difficult problem. It is common to treat a large gradient using a relatively small grid. Although, in principle, grid refinement can alleviate this problem, the necessary degree of refinement is often totally impractical, especially if one is attempting to model high-speed three-dimensional turbulent flow. In order to avoid this difficulty, it is necessary to seek a relation between the turbulence dissipation rate and other turbulence quantities. It is the key point in this study. In view of the definition of the eddy viscosity coefficients that are the ratio of the shear stress to the mean wind shear, one can write the following equations:

$$K_{xz}=\overline{-u'w'}\Big/\frac{\partial\bar{u}}{\partial z}, \tag{15}$$

$$K_{yz}=\overline{-v'w'}\Big/\frac{\partial\bar{v}}{\partial z}. \tag{16}$$

Thus, Eqs. (11) and (12) result in

$$K_m=K_{xz}=K_{yz}=\left(\frac{C_6-C_2}{C_1}\right)\frac{e^2}{\epsilon}. \tag{17}$$

It is readily seen from (17) that the relationship between the turbulence dissipation rate and eddy viscosity coefficient for the momentum can be applied to solve the difficulty mentioned before. Here K_{xz} and K_{yz} are equal in agreement with Shir's (1973) results.

By differentiating (17) with respect to time, we obtain

$$\frac{DK_m}{Dt}=\frac{2K_m}{e}\frac{De}{Dt}-\frac{K_m}{\epsilon}\frac{D\epsilon}{Dt}. \tag{18}$$

Substituting Eqs. (13) and (14) into (18), the proposed dynamic equation for the eddy viscosity coefficient can be written as

$$\frac{DK_m}{Dt}=(2-C_8)\frac{K_m}{e}\left(-\overline{u'w'}\frac{\partial\bar{u}}{\partial z}-\overline{v'w'}\frac{\partial\bar{v}}{\partial z}\right)+C_0(C_9-2)e+\left(\frac{2C_6(1+C_6)C_7}{C_0}\right)\frac{K_m}{e}\frac{\partial}{\partial z}\left(K_m\frac{\partial e}{\partial z}\right)-C_6C_{10}\frac{K_m}{\epsilon}\left[2\frac{\partial}{\partial z}\left(e\frac{\partial e}{\partial z}\right)-\frac{1}{C_0}\frac{\partial}{\partial z}\left(\epsilon\frac{\partial K_m}{\partial z}\right)\right], \tag{19}$$

where $C_0=(C_6-C_2)/C_1$ and C_8, C_9 and C_{10} are constants used for determination of K_m. The advantages of this dynamic formulation for K_m are that the vertical variation for K_m is much slower than ϵ and the boundary condition on K_m near the surface is easier to treat. Hence, Eq. (19) is a good substitution for Eq. (14).

c. Determination of the constants

It is seen that Eqs. (11)–(14) and Eq. (19) involve many undetermined constants C_i, some of which can be determined from measurements in simple turbulent flows or by reference to the properties of the constant-flux layer. For example, C_1 lies between 2.5 and 3.0 according to measurement data in the absence of mean strain. The value $C_1=2.8$ which is suggested by Hanjalic and Launder (1972) is chosen for this study. Since C_1 is a known value, we can reduce to a set of algebraic equations by neglecting advection and diffusion terms in (6) for the constant-flux layer. Therefore, we have

$$-2\overline{u'w'}\frac{\partial\bar{u}}{\partial z}-2.8\frac{\epsilon}{e}\left(\overline{u'^2}-\frac{2e}{3}\right)-\tfrac{2}{3}\epsilon=0, \tag{20a}$$

$$-2.8\frac{\epsilon}{e}\left(\overline{v'^2}-\frac{2e}{3}\right)-\tfrac{2}{3}\epsilon=0, \tag{20b}$$

$$-2.8\frac{\epsilon}{e}\left(\overline{w'^2}-\frac{2e}{3}\right)-\tfrac{2}{3}\epsilon=0, \tag{20c}$$

$$-(\overline{w'^2}-C_2e)\frac{\partial\bar{u}}{\partial z}-2.8\frac{\epsilon}{e}\overline{u'w'}=0, \tag{20d}$$

$$\overline{v'w'}=0, \tag{20e}$$

$$\overline{u'v'}=0. \tag{20f}$$

Eqs. (20b) and (20c) may be written, after some algebra, as

$$\overline{v'^2}=0.43e, \tag{20}$$

$$\overline{w'^2}=0.43e. \tag{21}$$

Then the constant C_6 mentioned before which is the ratio of normal stress $\overline{w'^2}$ to turbulence kinetic energy e is equal to 0.43 as indicated in Eq. (21). This constant C_6 obtained by Mellor (1973) has the value of 0.46. Since $2e=\overline{u'^2}+\overline{v'^2}+\overline{w'^2}$, we obtain $\overline{u'^2}=1.14\ e$. Substituting $\overline{u'^2}$ into (20a), we have

$$\epsilon=\overline{-u'w'}\frac{\partial\bar{u}}{\partial z}. \tag{22a}$$

It follows from Eqs. (22a) and (20d) that C_2 has the form of

$$C_2=0.43-2.8\left(\frac{\overline{-u'w'}}{e}\right)^2. \tag{22b}$$

TABLE 1. The values of the constants.

C_1	C_2	C_3	C_4	C_5	C_6	C_7	C_8	C_9	C_{10}
2.8	0.318	1.0	2.0	2.8	0.43	0.11	0.04	0.08	0.112

If the value of $-\overline{u'w'}/e=0.328$ (Mellor, 1973) is used, we obtain $C_2\approx0.129$. By choosing $-\overline{u'w'}/e\approx0.2$ near the surface (Shir, 1973), we find that $C_2\approx0.318$.

For the decay of homogeneous isotropic turbulence with zero strain at large Reynolds numbers, we require $C_4=2.0$ which is confirmed by Reynolds (1970). And for the homogeneous turbulent flow, C_3 is shown to be equal to 1.0 (Reynolds, 1970). The values of C_5 and C_7 could be estimated from computer optimization and the values for C_8, C_9 and C_{10} can be obtained from (18) once the constants are determined in (13) and (14). Then these estimated constants are corrected to obtain realistic results. The values of the constants used in this study are listed in Table 1.

d. Numerical technique and boundary conditions

On account of highly nonlinear terms in the model equations described previously and no exact functional approach to their solutions, the Galerkin residual technique is normally applied. For simplicity, the one-dimensional solutions are considered in this study. The model equations are normalized by expressing the parameters and variables x, z, t, f_1, $\bar{u}$, $\bar{v}$, e, ϵ, $-\overline{u'w'}$, $\overline{v'w'}$ in terms of $H\hat{x}$, $H\hat{z}$, $H\hat{t}/u_*$, u_*F/H, $u_*\hat{\bar{u}}$, $u_*\hat{\bar{v}}$, $u_*^2\hat{e}$, $u_*^3\hat{\epsilon}/H$, $-u_*^2\widehat{\overline{u'w'}}$ and $u_*^2\widehat{\overline{v'w'}}$, respectively. Here H is the height of the model and u_* is the frictional velocity. The quantities with a caret and the capital F are nondimensional. Then the new dimensionless form of the model equations is identical with its original form. For abbreviation, we shall drop the caret in the nondimensional model equations for later analysis. Hence, the nondimensional model equations are solved by the Galerkin finite element technique. Within a typical element, for example, the variables $\bar{u}$, $\bar{v}$, e, ϵ and K_m are approximated by $\tilde{\bar{u}}$, $\tilde{\bar{v}}$, $\tilde{e}$, $\tilde{\epsilon}$ and $\tilde{K}_m$. Thus, we have

$$\left.\begin{aligned}\bar{u}\approx\tilde{\bar{u}}=[N]\{\bar{u}\},\quad \bar{v}\approx\tilde{\bar{v}}=[N]\{\bar{v}\},\quad e\approx\tilde{e}=[N]\{e\}\\ \epsilon\approx\tilde{\epsilon}=[N]\{\epsilon\},\quad K_m\approx\tilde{K}_m=[N]\{K_m\}\end{aligned}\right\},\tag{23}$$

where the shape function $[N]$ is assumed to be a linear interpolation and to refer to individual nodes in which the function N_i referring to node i takes on unit value at node i and zero value at all the other nodes of the element. The functions $\{\bar{u}\}$, $\{\bar{v}\}$, $\{e\}$, $\{\epsilon\}$ and $\{K_m\}$ are undetermined coefficients that are the model solutions at specified points (or nodes) in the computed domain. For the time being, the same shape functions are used for all independent variables. After introduction of these functions [Eq. (23)] into the model equations and enforcing the resultant equations to shape function orthogonally, one can finally obtain a system of ordinary differential equations. A detailed description of the finite-element solution of the model equations is discussed in the Appendix.

At the top of the boundary layer, the following conditions prevail:

$$\frac{\partial\bar{u}}{\partial z}=\frac{\partial\bar{v}}{\partial z}=0;\quad e=\epsilon=0;\quad -\overline{u'w'}=\overline{v'w'}=0.\tag{24}$$

For K_m at the top of the boundary layer, it is not clear now from Eq. (17) whether K_m should be zero or not since e and ϵ are assumed to be zero. However, there is very little difference in the results between a fixed small value and we thus set zero for K_m.

At the bottom of the boundary layer, we assume

$$\left.\begin{aligned}-\overline{u'w'}=1,\quad \overline{v'w'}=0,\quad e=-\overline{u'w'}/0.2\\ \bar{v}=0,\quad K_m=0.04\frac{e^2}{\epsilon}\end{aligned}\right\},\tag{25}$$

where $\epsilon=-\overline{u'w'}\partial\bar{u}/\partial z$. In order to handle the rapid variation of $\bar{u}$-mean wind near the surface (Shir, 1973), we take the form of

$$\bar{u}=\frac{1}{k}\ln\left(\frac{Hz}{Z_0}\right)\quad\text{at } z=0.01,\tag{26}$$

where k is the von Kármán constant and Z_0 is the surface roughness.

4. Numerical results

In order to compare Deardorff's and Shir's results, $F=Hf_1/u_*=0.455$ which is the height of the PBL indicated by Deardorff and $H/Z_0=0.455\times10^5$ which is taken for the computation in Shir's model are used for this study. The whole boundary layer consists of 65 grid points in which fine meshes near the surface in the vertical are taken.

a. Mean wind profiles

Fig. 1 shows the vertical mean wind profiles of $\bar{u}$ and $\bar{v}$. The negative $\bar{v}$ component mean wind is due to the orientation of the coordinate of which the x coordinate is along the surface mean wind and the z coordinate is vertically perpendicular to the surface mean wind.

b. Reynolds stresses

The computed Reynolds stresses $-\overline{u'w'}$ and $\overline{v'w'}$ are shown in Fig. 2. It shows very good agreement between our simple model results using the finite-element technique and Deardorff's or Shir's sophisticated model results using the finite-difference scheme.

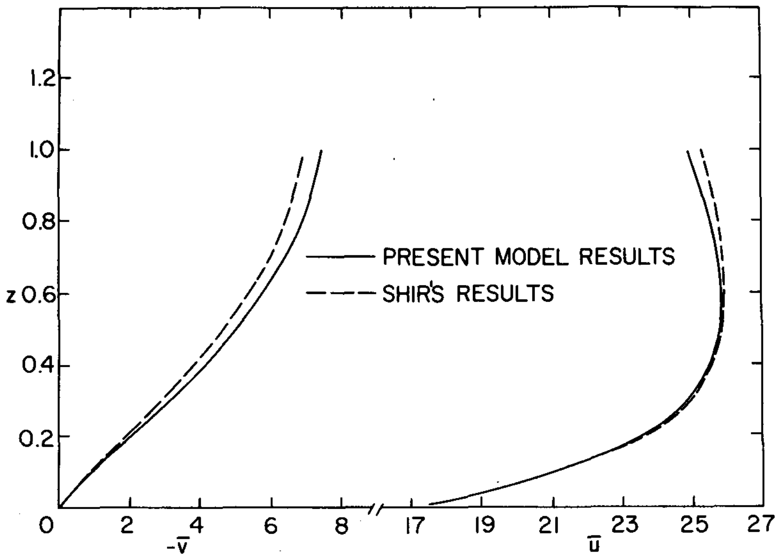

FIG. 1. Vertical profiles of the mean wind ($\bar{u}$, $\bar{v}$).

c. Turbulence kinetic energy and sum of horizontal shear stresses

Fig. 3 shows the computed turbulence kinetic energy (e) and the sum of horizontal shear stresses $(-\overline{u'w'}^2+\overline{v'w'}^2)^{\frac{1}{2}}$. The ratio between them is about 0.2. It means that the sum of horizontal shear stresses is 10% of the sum of the normal stresses. This property may prove useful for simplifying the complicated turbulence model in order to have a simple dynamic turbulence model suitable for the neutral atmospheric planetary boundary layer.

d. Turbulence dissipation rate

Fig. 4 shows the computed turbulence dissipation rate. A rapid decrease upward for turbulence dissipation rate near the surface is shown. As noted earlier, the use of a relatively small grid to treat such a large gradient of turbulence dissipation rate near the surface is impractical. Hence, a dynamic equation for the eddy viscosity coefficient is written in substitution for the equation of the turbulence dissipation rate.

e. Eddy viscosity coefficient for momentum

The vertical profile of the eddy viscosity coefficient for momentum is plotted in Fig. 5 in comparison with the result of Shir's model. The profile from the present model shows a maximum value near one-third of the height of the PBL, which bears resemblance to that proposed by O'Brien (1970). It is noted that the present

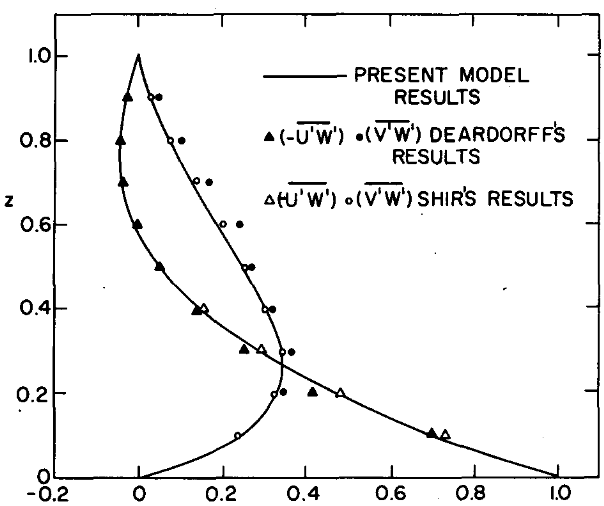

FIG. 2. Vertical profiles of the Reynolds' stresses.

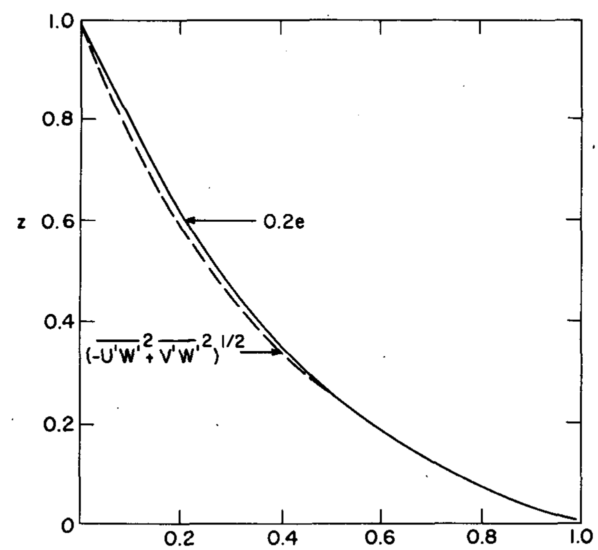

FIG. 3. Vertical profiles of the turbulence kinetic energy and the sum of horizontal shear stresses.

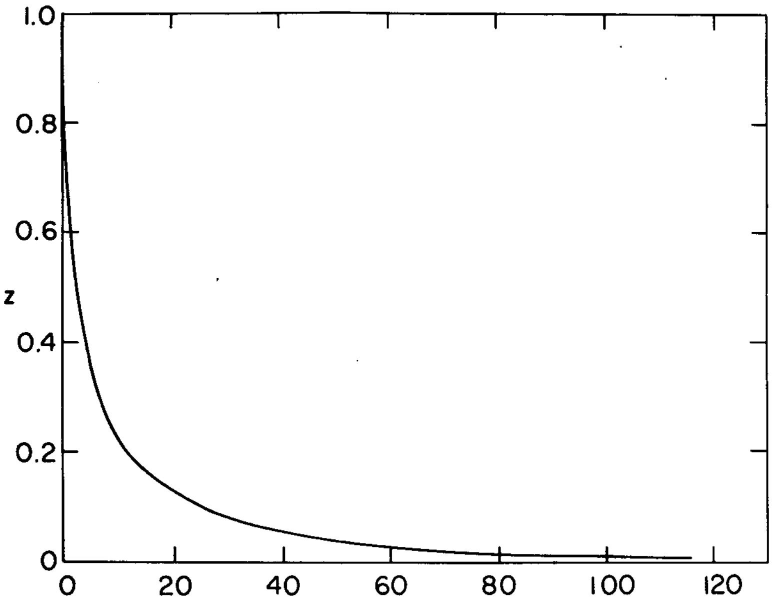

FIG. 4. Vertical profiles of the turbulence dissipation rate.

model does not have the difficulties in which the eddy coefficients become indeterminate if there are small values of mean wind shears and Reynolds stresses.

f. Turbulence length scale

There seems to be universal agreement that the turbulence length scale should be expressed by

$$l=C\frac{e^{1.5}}{\epsilon}, \quad (27)$$

where the constant C depends on the specific scales and flow (0.055 is chosen for this computation). Then the computed vertical profile of the turbulence length scale using (27) is shown in Fig. 6. At $z=1.0$ it is not clear now whether l should be zero or not because the turbulence dissipation rate and the turbulence kinetic energy both approach zero at that height. The turbulence length scale computed from the present model agrees quite well with Blackadar's data (1962).

5. Discussion and conclusion

A simple turbulent closure dynamic model which is suitable for simulation of the neutral atmospheric planetary boundary layer has been presented, using the finite-element technique. The high-order closure scheme has emphasized the need for studying the structures of the turbulent motion in the lower atmo-

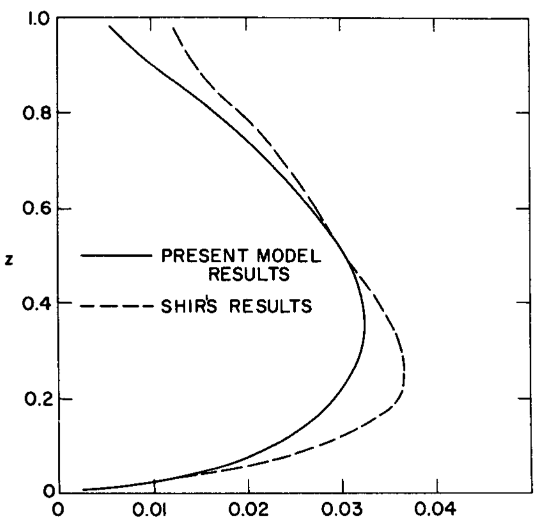

FIG. 5. Vertical profiles of the eddy viscosity coefficient for momentum.

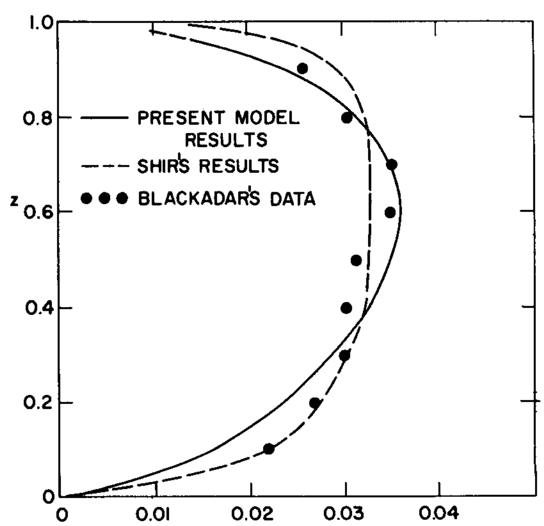

FIG. 6. Vertical profiles of the turbulence length scale.

sphere. It is noted that the high-order closure scheme does not need any information about eddy viscosity coefficients which is required by the first-order closure scheme. However, the second-order closure scheme can be used to determine the eddy viscosity coefficients and this approach has been taken here. In preliminary results, the behavior of the neutral PBL agrees well with the available data and with the existing elaborate turbulent models, using a finite-difference scheme. Due to the advantages of accurate representation of complex geometry with the finite-element method, the numerical technique could be extended to treat nonhomogeneous turbulence. The dynamic formulation of the eddy viscosity coefficient for momentum is particularly attractive and can provide a viable alternative approach to study atmospheric turbulence, diffusion and air pollution. Especially in studying the air pollution over a mountain, it is important to determine the eddy viscosity coefficients in order to solve an advection-diffusion equation if the gradient transport theory is applied.

Acknowledgments. This research was supported by the Division of Biomedical and Environmental Research, U.S. Department of Energy, under Contract EY-76-S-02-2455 and by the National Aeronautics and Space Administration, under Contract NAS 6-2498.

APPENDIX

Finite Element Solution

For simplicity, the planetary boundary layer is characterized by horizontal homogenity in the wind and turbulence fields. Then Eqs. (8)–(17) can be written in nondimensional form as follows:

$$\frac{\partial \bar{u}}{\partial t}-F(\bar{v}-\bar{v}_g)-\frac{\partial}{\partial z}\left(K_m\frac{\partial \bar{u}}{\partial z}\right)=0 \qquad \text{(A1)}$$

$$\frac{\partial \bar{v}}{\partial t}+F(\bar{u}-\bar{u}_g)-\frac{\partial}{\partial z}\left(K_m\frac{\partial \bar{v}}{\partial z}\right)=0 \qquad \text{(A2)}$$

$$\frac{\partial e}{\partial t}-K_m\left[\left(\frac{\partial \bar{u}}{\partial z}\right)^2+\left(\frac{\partial \bar{v}}{\partial z}\right)^2\right] -\left[\frac{C_1C_6(1+C_6)C_7}{C_6-C_2}\right]\frac{\partial}{\partial z}\left(K_m\frac{\partial e}{\partial z}\right)+\epsilon=0 \qquad \text{(A3)}$$

$$\frac{\partial \epsilon}{\partial t}-C_3\left(\frac{C_6-C_2}{C_1}\right)e\left[\left(\frac{\partial \bar{u}}{\partial z}\right)^2+\left(\frac{\partial \bar{v}}{\partial z}\right)^2\right] +C_4\frac{\epsilon^2}{e}-\left(\frac{C_1C_6C_5}{C_6-C_2}\right)\frac{\partial}{\partial z}\left(K_m\frac{\partial \epsilon}{\partial z}\right)=0 \qquad \text{(A4)}$$

$$K_m=\left(\frac{C_6-C_2}{C_1}\right)\frac{e^2}{\epsilon}. \qquad \text{(A5)}$$

Taking derivatives in Eqs. (A1) and (A2), we have

$$\frac{\partial S}{\partial t}-FW-\frac{\partial^2}{\partial z^2}(K_mS)=0, \qquad \text{(A6)}$$

$$\frac{\partial W}{\partial t}+FS-\frac{\partial^2}{\partial z^2}(K_mW)=0, \qquad \text{(A7)}$$

in which the geostrophic wind $(\bar{u}_g,\bar{v}_g)$ disappears and the wind shears are

$$S=\frac{\partial \bar{u}}{\partial z},\quad W=\frac{\partial \bar{v}}{\partial z}. \qquad \text{(A8)}$$

The model equations described above are highly nonlinear and there is no exact functional approach to their solutions. The Galerkin finite-element technique is usually taken to derive the element equation. Within a typical element, we assume

$$\left.\begin{array}{lll} S=[N]\{S\} & W=[N]\{W\} & e=[N]\{e\} \\ \epsilon=[N]\{\epsilon\} & K_m=[N]\{K_m\} & \end{array}\right\}, \qquad \text{(A9)}$$

where the square brackets represent a row vector or rectangular or square matrix and the braces represent a column vector. The same shape functions $[N]$ are used for all variables. After introduction of these functions into the model equations and enforcing them to shape function orthogonally, one obtains for an element over domain Ω

$$[D]\{\dot{S}\}-[A]\{W\}+[B]\{S\}=0, \qquad \text{(A10)}$$

$$[D]\{\dot{W}\}+[A]\{S\}+[B]\{W\}=0, \qquad \text{(A11)}$$

$$[D]\{\dot{e}\}+[C]\{e\}+[D]\{\epsilon\}-\{E\}=0, \qquad \text{(A12)}$$

$$[D]\{\dot{\epsilon}\}-[G]\{e\}+[H]\{\epsilon\}=0, \qquad \text{(A13)}$$

where

$$[A]=\int_\Omega F[N]^T[N]d\Omega, \qquad \text{(A14)}$$

$$[B]=\int_\Omega ([N_z]^T[N]\{K_m\}^*[N_z] +[N_z]^T[N][N_z]\{K_m\}^*)d\Omega, \qquad \text{(A15)}$$

$$[C]=\int_\Omega \left(\frac{C_1C_6(1+C_6)C_7}{C_6-C_2}\right) \times[N_z]^T[N]\{K_m\}^*[N_z]d\Omega, \qquad \text{(A16)}$$

$$[D]=\int_\Omega [N]^T[N]d\Omega, \qquad \text{(A17)}$$

$$\{E\}=\int_\Omega [N]^T[N]\{K_m\}^*(([N]\{S\}^*)^2$$

$$+([N]\{W\}^*)^2)d\Omega, \quad \text{(A18)}$$

$$[G]=\int_\Omega C_3\left(\frac{C_6-C_2}{C_1}\right)[N]^T[N]\left(([N]\{S\}^*)^2 + ([N]\{W\}^*)^2\right)d\Omega, \quad \text{(A19)}$$

$$[H]=\int_\Omega \left(C_4[N]^T[N]\{g\}^*[N] + \left(\frac{C_1C_6C_5}{C_6-C_2}\right)[N_z]^T[N]\{K_m\}^*[N_z]\right)d\Omega, \quad \text{(A20)}$$

in which $g=\epsilon/e$ and asterisk represents the last computed nodal values of the variables. $[\ ]^T$ denotes the transpose of a matrix and the dots in (A10)–(A13) denote differentiation with respect to time. Thus, (A10)–(A13) are solved successfully by using the last nodal values of S, W, e, ϵ and K_m to update $[B]$, $[C]$, $\{E\}$, $[G]$ and $[H]$. In order to increase computational stability and to reduce core storage requirements which increase dramatically with the number of variables computed and the dimension of problem solved, the model equations evaluate sequentially but not simultaneously. First, we compute S and W from wind shear equations (A10) and (A11). Second, using the new values of S and W, we calculate e and ϵ from turbulence kinetic energy equation (A12) and turbulence dissipation rate equation (A13). Third, based on Eqs. (11), (12) and (A5), we get $-\overline{u'w'}$, $\overline{v'w'}$ and K_m. Fourth, integrating numerically the wind shears S and W, we obtain $\bar{u}$ and $\bar{v}$. The process is then repeated until very little change occurs in the variables. Similarly, the procedure is applied to the model equations which involve (19) instead of (A4). The computational results through the model equations involving either (19) or (A4) are very close to each other. For the time being, due to little application of the finite-element numerical technique to the solution of turbulent flow predictions, solutions which are considerably more common are the steady-state solutions which are presented here.

REFERENCES

Baker, A. J., 1978: Finite element analysis of turbulent flow. *Proceedings of the International Conference On Numerical Methods In Laminar and Turbulent Flow*, University College Swansea, Pentech Press, London, 203–230.

Blackadar, A. K., 1962: The vertical distribution of wind and turbulent exchange in a neutral atmosphere. *J. Geophys. Res.*, **67**, 3095–3102.

Deardorff, J. W., 1970a: A three-dimensional numerical investigation of the idealized planetary boundary layer. *Geophys. Fluid Dyn.*, **1**, 377–410.

——, 1970b: A numerical study of three-dimensional turbulent channel flow at large Reynolds numbers. *J. Fluid Mech.*, **41**, 453–480.

Freeman, B. E., 1977: Tensor diffusivity of a trace constituent in a stratified boundary layer. *J. Atmos. Sci.*, **34**, 124–136.

Frost, W., W. L. Harper and G. H. Fichtl, 1974: Analysis of atmospheric flow over a surface protrusion using the turbulence kinetic energy equation. *Bound.-Layer Meteor.*, **8**, 401–417.

Hanjalic, D., and B. E. Launder, 1972: A Reynolds stress model of turbulence and its application to thin shear flows. *J. Fluid Mech.*, **52**, 609–638.

Huebner, K. H., 1975: *The Finite Element Method for Engineers.* Wiley, 500 pp.

Jackson, P. S., and J. C. R. Hunt, 1975: Turbulent wind flow over a low hill. *Quart. J. Roy. Meteor. Soc.*, **101**, 929–955.

Martin, H. C., and G. F. Carey, 1973: *Introduction To Finite Element Analysis Theory and Application.* McGraw-Hill, 386 pp.

Mellor, G., 1973: Analytic prediction of the properties of stratified planetary layers. *J. Atmos. Sci.*, **30**, 1061–1069.

——, and H. J. Herring, 1973: A Survey of the mean turbulent field closure models. *AIAA J.*, **11**, 590–599.

——, and Yamada, 1974: A hierarchy of turbulence closure models for planetary boundary layer. *J. Atmos. Sci.*, **31**, 1791–1806.

Lee, H. N., 1979: Atmospheric turbulence and diffusion boundary layer transport model. *Preprints Fourth Symp. Turbulence, Diffusion and Air Pollution*, Reno, Amer. Meteor. Soc., 471–476.

O'Brien, J. J., 1970: A note on the vertical structure of the eddy exchange coefficient in the planetary boundary layer. *J. Atmos. Sci.*, **27**, 1213–1215.

Reynolds, W. C., 1970: Computation of turbulent flow state-of-the-art. Rep. MD-27, Thermosciences Div., Dept. of Mech. Eng., Stanford University, 90 pp.

Schamber, D. R., and Larock, B. E., 1978: Computational aspects of modelling turbulent flows by finite elements. *Proceedings of the International Conference On Numerical Methods In Laminar and Turbulent Flow*, University College Swansea, Pentech Press, London, 245–256.

Shir, C. C., 1973: A preliminary numerical study of atmospheric turbulent flow in the idealized planetary boundary layer. *J. Atmos. Sci.*, **30**, 1327–1339.

——, and R. D. Bornstein, 1977: Eddy exchange coefficients in numerical models of the planetary boundary layer. *Bound.-Layer Meteor.*, **11**, 171–185.

Taylor, P. J., and P. R. Gent, 1974: A model of atmospheric boundary layer flow above gentle topography. *Bound.-Layer Meteor.*, **7**, 349–362.

Wyngaard, J. C., and O. R. Cote, 1974: The evolution of a connective planetary boundary layer—A higher-order-closure model study. *Bound.-Layer Meteor.*, **7**, 289–308.

Yamada, T., and Mellor, G., 1975: A simulation of the Wangara atmospheric boundary layer data. *J. Atmos. Sci.*, **32**, 2309–2329.